

TOWARDS ENHANCING VOLTAGE STABILITY AND POWER LOSS REDUCTION OF A TRANSMISSION SYSTEM: A COMPARATIVE SURVEY OF THE IMPACT OF FACTS CONTROLLERS ON 330KV NIGERIA TRANSMISSION SYSTEM

Etim, Archibong A.a*, Akpama, E. J.b, Peter O. Ohiero c

a,b,c Department of Electrical and Electronic Engineering, University of Cross River State, Calabar, Nigeria,

*Correspondence Author: <u>archibongetim322@gmail.com</u>

Received: 15th August, 2024 Reviewed: 27th August, 2023 Accepted: 19th September, 2024

Abstract.

Electrical power transmission is one of the developmental keys of a nation. Due to the significantly increasing of industrial growth, high power transmission demands, and poor performance of power systems in Nigeria, voltage instability is gaining more attention and has become a challenging problem leading to voltage collapse of power systems. The purpose of this paper is to compare the effectiveness of three FACTS Controllers: Static Var Compensator (SVC), Static Synchronous Compensator (STATCOM), and Thyristor Control Series Compensator (TCSC) on the impact of voltage stability enhancement and power loss reduction of the transmission line. To achieve this, the 52-bus network and each FACTS controller were modeled and simulated, and load flow analysis was carried out by Adaptive Newton Raphson with 99 iterations using ETAP environment. From the simulation, weak and weakest buses were detected and solutions were obtained for each FACTS controller used in the test system as three separate test cases. The result obtained can eventually help in concluding the effectiveness of each controller with respect to voltage profile improvement and power loss reduction in the power system.

 $\textbf{Keywords} \hbox{: } Controllers, Power System Planning, Compensations, Stability, Voltage Profile.$

I. INTRODUCTION

Voltage Stability analysis is important as voltage instability may result in the partial or complete interruption in the power system. For voltage stability analysis, a number of steady-state analysis methods such as standard power flow methods, continuation power flow methods, modal methods and dynamic simulation methods are being used by the electric utilities. [1] The reactive power plays an important role in a power system. Fundamentally, an electric power is generated, transmitted and then distributed to the customers. [2,3] Transformers, transmission and distribution lines, cables and many common load devices such as motors shift the relationship between current and voltage due to their inherent characteristics. This shift is measured in Volt

Ampere Reactive (VAR). High VAR levels may result in a reduction in power transfer capability and an increase in losses. Low VAR levels may result in voltage sag. Hence, appropriate levels of reactive power are to be maintained to enhance the voltage stability of the power system [3]. The sources of reactive power such as conventional devices which are built out of resistance, inductance or capacitance together with a transformer, and Flexible AC Transmission System (FACTS) devices provide sufficient reactive power to the system [4, 5, 6, 7, 8]. FACTS devices provide reactive power compensation and improve voltage stability, transmission capability, power flow control, and operating flexibility of the power system. The purpose of this research is to provide an analysis of the use of FACTS devices in improving voltage stability,

minimizing power loss, and improving transmission system loadability that result from utilization of different types of shunt and series FACTS devices such as Static Voltage Compensator (SVC), Static Synchronous Compensator (STATCOM), and Thyristor Controlled Series Compensator (TCSC). To test the idea, we have introduced different FACTS devices into the IEEE 39 bus New England test system. Voltage stability of the power system before and after introducing the different FACTS devices is observed by comparing metrics such as active and reactive power losses, voltage magnitude profile, loading margin, and P-V curves [9,10]. In modern power transmission system, voltage downfall aspect has become crucial concerns over the decades as it is being a major cause for numerous series power failure that have encountered throughout the world. Nowadays, electricity plays a significant role in the development of any economy and the inadequate supply of electricity to meet the ever-growing demand of power has caused power system to operate under highly stressed conditions. The electricity demand is increasing day by day with the technological developments. This increasing energy demand in turn have led to the difficulty in maintaining the system voltages within the acceptable limit and therefore driving the power system to work near the boundary of instability margin thus, creates the problem of voltage stability in power systems. Voltage stability refers to the ability of a power system to maintain steady voltages at all the buses in the system after being subjected to a disturbances from a given initial operating condition [11, 12]. The power system voltage is stable if voltages after disturbances are close to voltages at normal operating conditions. A power system becomes unstable when voltage uncontrollably decreases due to outage of equipment and sudden increment in load. Voltage stability is generally a local problem, but the consequences of voltage instability have significant impact on the power system. The result of this impact is voltage failure arises when system is over loaded beyond its extreme load capability point. This effect leads to progressive and uncontrollable voltage drop in the system voltage and if no provision is given for an additional voltage support, system break down, voltage collapse and blackout may be experienced. Voltage stability has today become an important area receiving great attention from power system engineer and researchers. It is a serious problem, which steadily reaches operating limit, imposed by economic and environmental constraints. At the verge of voltage collapse, the rate of decrease of voltage will be so high giving no time for the operator respond. [11, 12,

Voltage collapse has occurred in many parts of the world due to inefficient voltage support. The major cause of voltage instability problem in power system is the inability of satisfy the reactive power demand at critical nodes in the power system. When the system is in a state of instability, voltage profile is affected and any drop in voltage profile is accompanied by increase in reactive power demand. If the reactive power demand is not met, it further causes decay of the bus voltage and this can lead to poor power transfer capability in the system with possible deficient equipment performance and damage. This therefore creates the need for compensating devices that can enhance and stabilize the system voltage profile by providing the required reactive power supports to the system. An important constrain regarded with the reactive power support is the installation of compensating devices at proper locations. [14] Reactive power must be provided at locations where its demand is the highest. If there happens to be excess reactive power in a power system, it causes two much heating and voltage drops. Therefore, the proper placing and sizing of reactive power generating devices is of prime importance. The most useful device that can produce the desired compensation for the system is the Flexible AC Transmission System (FACTS) [15, 16]. In power transmission system, the implementation of Flexible AC Transmission System (FACTS) devices is intensively preferred in order to minimize the Voltage instability, power losses and enhance power quality. According to the IEEE PES task force of the FACTS working group, the static VAR compensator can be defined as a shunt-connected static VAR generator or absorber whose output is adjusted to exchange capacitive or inductive current so as to maintain or control specific parameters of the electrical power system [17]. The SVC is built of power electronic devices such as the thyristor valve which is a stack of series connected anti-parallel thyristors to provide controllability, air core reactors, and high voltage AC capacitors and is connected to the transmission line through a power transformer. It includes a thyristorcontrolled reactor for leading VAR and a thyristorswitched capacitor for lagging VAR. The thyristorcontrolled reactor is defined by the IEEE PES task force of the FACTS working group as a "shunt-connected, thyristor-controlled inductor whose effective reactance is varied in a continuous manner by partial conduction control of the thyristor valve". The thyristor-switched capacitor is defined by the IEEE PES task force of the FACTS working group as a "shunt-connected, thyristorswitched capacitor whose effective reactance is varied in a stepwise manner by full- or zero-conduction operation of the thyristor valve" [18,19,20].

II. METHODOLOGY

Modeling of Typical Transmission Network:

The typical transmission line is presented as a line diagram shown in Figure 1

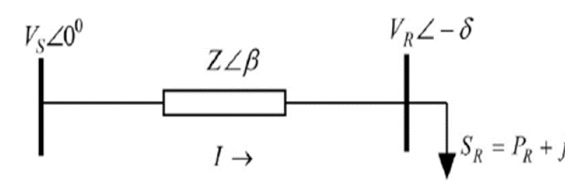


Figure 1: Single Line Diagram of Transmission Line

In the power system stability field, a particular interest is in controlling voltage and reactive power. The issue is to avoid voltage instability which can result in voltage collapse. Reactive power is very precious in keeping the system voltage stable [12, 17]. It is generated when the current waveform is not in phase with the voltage waveform because of energy-conserving elements like inductor or capacitors. Reactive power is required for reducing magnetic and electric fields in the inductor and capacitor respectively. The voltage in the transmission line can be varied with a variation of reactive power. This can be illustrated as follows:

$$S_R = P_R + jQ_R \tag{1}$$

Therefore, equation (1) may be expressed as,

$$S_R = V_R \left\{ \frac{V_S cos\delta + JV_S sin\delta - V_R}{JX} \right\}$$

$$S_R = \frac{V_R V_S sin\delta}{X} + J \frac{V_R V_S cos\delta - V_R^2}{X}$$
(2)

$$S_R = \frac{V_R V_S sin\delta}{X} + J \frac{V_R V_S cos\delta - V_R^2}{X}$$
 (3)

According to equation (3), the active and reactive power supplied to the load is:

$$P_R = \frac{V_R V_S \sin \delta}{X} \tag{4}$$

$$P_R = \frac{1}{X}$$

$$Q_R = \frac{V_R V_S cos \delta - V_R^2}{X}$$
(5)

From equation (4) and (5), using $\sin^2\theta + \cos^2\theta = 1$,

$$P_R^2 + (Q_R + \frac{V_R^2}{X})^2 = \frac{V_S^2 V_R^2}{X^2}$$
 (6)

The voltage at the receiving bus (bus-2) can be expressed

$$V_R^2 = \frac{1}{2} \left[V_S^2 - 2Q_R Z + V_S \left(\sqrt{V_S^2 - \frac{4P_R^2 Z^2}{V_S^2} - 4Q_R} \right) \right]$$
(7)

Where:

 V_S and V_R are bus voltages at the sending and receiving end respectively;

I is the line current, *X* is the reactant, δ is the generator's internal angle, P_S and P_R are active and reactive powers supplied to the load.

Formulation of Power Flow Equation in Transmission Network:

The power system network comprising nthbuses, the current I_i injected at the ith bus in the system is expressed as,

$$I_i = \sum_{k=1}^n Y_{ik} V_k; i = 1, 2 \dots n$$
 (8)

Where; I_i =the current on ith bus, V_k = the voltage at bus k, Y_{ik} = the admittance between bus i and bus k. The complex power injected by the source into ith bus is described as.

$$S_i = V_i I_i : i = 1, 2 \dots \dots n$$
(9)

$$S_i = P_i + jQ_i \tag{10}$$

Equations (9) and (10) are modified into two equations given as,

$$I_i = \frac{S_i^z}{V_i^*} \tag{11}$$

$$I_i = \frac{P_i - jQ_i}{V_i^*}$$

(12)

From equation (12),

$$P_i - jQ_i = V_i^* I_i \tag{13}$$

Substituting equation (8) we have,

$$P_i - jQ_i = V_i^* (\sum_{k=1}^n Y_{ik} V_k); i = 1, 2 \dots n$$
(14)

Separating equation (14) into imaginary and real components we have,

$$P_{i} = Re(V_{i}^{*}(\sum_{k=1}^{n} Y_{ik} V_{k}))$$
 (15)

$$\begin{aligned} P_i &= Re(V_i^*(\sum_{k=1}^n Y_{ik} V_k)) \\ Q_i &= -Im(V_i^*(\sum_{k=1}^n Y_{ik} V_k)) \end{aligned} \tag{15}$$

Where V_i, V_i^*, V_k and Y_{ik} are expressed in polar form as

$$V_{i} = |V_{i}|e^{j\delta_{i}}; V_{i}^{*} = |V_{i}^{*}|e^{-j\delta_{i}}; V_{k} = |V_{k}|e^{j\delta_{k}}; Y_{ik} = |Y_{ik}|e^{j\theta_{ik}}$$
(17)

Substituting equation (17) into equations (15) and (16), we have

$$\begin{array}{ll} P_{i} = & |V_{i}|\sum_{k=1}^{n}|Y_{ik}||V_{k}|\cos{(\theta_{ik}+\delta_{k}-\delta_{i})}\\ Q_{i} = & -|V_{i}|\sum_{k=1}^{n}|Y_{ik}||V_{k}|\sin{(\theta_{ik}+\delta_{k}-\delta_{i})} \end{array}$$

Equations (18) and (19) are static power flow equations that produce a total of 2n power equations. The equations are non-linear and therefore Newton Raphson method is adopted for accuracy, reliability, and faster rate of convergence. The Newton-Raphson power flow is expressed by:

$$\begin{bmatrix} \Delta P \\ \Delta Q \end{bmatrix} = \begin{bmatrix} J_1 & J_2 \\ J_3 & J_4 \end{bmatrix} \begin{bmatrix} \Delta \delta \\ \Delta V \end{bmatrix}$$
 (20)

Where; ΔP is the real power mismatch, ΔQ is the reactive power mismatch, $\Delta\delta$ is the bus voltage mismatch. J_1, J_2, J_3 and J_4 are the elements of the Jacobian matrix which are obtained by partial differentiation of equations (18) and (19) concerning the static variables (δ , V). The off-diagonal and diagonal matrix of J_1, J_2, J_3 and J_4 are expressed as follows:

The off-diagonal and diagonal matrix of J_1 :

$$\frac{\partial P_i}{\partial \delta_k} = V_i V_k Y_{ik} \sin(\theta_{ik} + \delta_i - \delta_k), k \neq i$$
(21)
$$\frac{\partial P_i}{\partial \delta_k} = -\sum_{k=1}^{n} V_i V_k Y_{ik} \sin(\theta_{ik} + \delta_i - \delta_k)$$
(22)

The off-diagonal and diagonal matrix of I_2 :

$$\frac{\partial P_i}{\partial V_k} = V_i Y_{ik} \cos(\theta_{ik} + \delta_i - \delta_k), k \neq i$$
 (23)

$$\frac{\partial P_i}{\partial V_k} = 2V_i Y_{ii} \cos \theta_{ii} + \sum_{\substack{k=1 \ k=i}}^{n} V_k Y_{ik} \cos(\theta_{ik} + \delta_i - \delta_k)$$
(24)

The off-diagonal and diagonal matrix of I_3 :

$$\frac{\partial Q_i}{\partial \delta_k} = -V_i V_k Y_{ik} \cos(\theta_{ik} + \delta_i - \delta_k), k \neq i$$

$$\frac{\partial P_i}{\partial \delta_i} = \sum_{\substack{k=1\\k=i}}^n V_i V_k Y_{ik} \cos(\theta_{ik} + \delta_i - \delta_k)$$
(26)

The off-diagonal and diagonal matrix of J_4

$$\frac{\partial Q_i}{\partial V_k} = V_i Y_{ik} \sin(\theta_{ik} + \delta_i - \delta_k), k \neq i$$

(27) $\frac{\partial Q_i}{\partial V_i} = 2V_i Y_{ii} \sin \theta_{ii} + \sum_{\substack{k=1 \ k=i}}^{n} V_k Y_{ik} \sin(\theta_{ik} + \theta_{ik})$

$$\delta_i - \delta_k \tag{28}$$

The real and reactive power mismatches at each iteration with new estimates of the bus voltage angles and voltage magnitude are expressed as follows:

$$\Delta P_{i}^{r} = P_{i}^{s} - P_{i}^{r}$$

$$\Delta Q_{i}^{r} = Q_{i}^{s} - Q_{i}^{r}$$

$$\delta_{i}^{r+1} = \delta_{i}^{r} - \Delta \delta_{i}^{r}$$

$$V_{i}^{r+1} = V_{i}^{r} - \Delta V_{i}^{r}$$
(32)

$$\Delta Q_i^r = Q_i^s - Q_i^r \tag{30}$$

$$\delta_i^{r+1} = \delta_i^r - \Delta \delta_i^r \tag{31}$$

$$V_i^{r+1} = V_i^r - \Delta V_i^r \tag{32}$$

Where, r is the iteration count, ΔP_i^r is the real power mismatch at r-iteration, P_i^s is the special value of real power, P_i^r is the calculated value of real power at riteration, ΔQ_i^r is the reactive power mismatch at r iteration, Q_i^s is the special value of reactive power, Q_i^r is the calculated value of reactive power at r-iteration, $\delta_i^{r+1} = \delta_i^r - \Delta \delta_i^r$; $V_i^{r+1} = V_i^r - \Delta V_i^r$, δ_i^{r+1} is the new estimate of bus angle at iteration r+1, δ_i^r is the calculated value of the bus voltage angle at r-iteration, $\Delta \delta_i^r$ is the bus voltage angle mismatch at r-iteration, V_i^{r+1} is the new estimate of bus voltage at iteration r+1, V_i^r is the calculated value of the bus voltage at r-iteration, ΔV_i^r is the bus voltage mismatch at r-iteration. The voltage and reactive power constraints at each bus i are expressed as follows:

$$V_{i(min)} \le V_i \le V_{i(max)}$$
(33)
$$Q_{i(min)} \le Q_i \le Q_{i(max)}$$
(34)

 $V_{i(min)}$ and $V_{i(max)}$ are the minimum and Where; maximum voltage values at bus i;

> $Q_{i(min)}$ and $Q_{i(max)}$ are the minimum and maximum reactive power supplied at bus i;

Modeling and Formulation of Power Flow of Static Var Compensator (SVC)

. The equivalent circuit of this model is shown in Figure 2

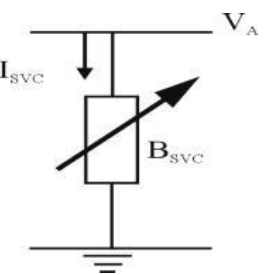


Figure 2: Variable shunt susceptance model of **SVC**

The current and reactive power equation along with the linearized Newton-Raphson power flow equation for SVC model are expressed as follows:

$$I_{svc} = B_{svc}V_K$$

$$(52)$$

$$Q_{svc} = Q_k = -V_k^2 B_{svc}$$

$$\begin{bmatrix} \Delta P_k \\ \Delta Q_k \end{bmatrix}^{(r)} = \begin{bmatrix} 0 & 0 \\ 0 & Q_k \end{bmatrix}^{(r)} \begin{bmatrix} \Delta \delta_k \\ \Delta B_{svc} / B_{svc} \end{bmatrix}^{(r)}$$

(54)

$$B_{svc}^{(r)} = B_{svc}^{(r-1)} + \left(\frac{\Delta B_{svc}}{B_{svc}}\right)^{(r)} B_{svc}^{(r-1)}$$
 (55)

Where:

 I_{SPC} is the current drawn by SVC;

 B_{svc} is the variable shunt susceptance of SVC;

 Q_{SVC} is the reactive power drawn by SVC;

 ΔB_{svc} is the variable shunt susceptance mismatch of SVC

The susceptance and reactive power equations along with the linearized Newton-Raphson power flow equation for this model is expressed as follows:

$$B_{svc} = \frac{-\left[X_L - \frac{X_C}{\pi} \{2(\pi - \alpha_{svc}) + \sin{(2\alpha_{svc})}\}\right]}{X_C X_L}$$
(56)
$$Q_{svc} = Q_k = \frac{V_k^2 \left[X_L - \frac{X_C}{\pi} \{2(\pi - \alpha_{svc}) + \sin{(2\alpha_{svc})}\}\right]}{X_C X_L}$$
(57)
$$\begin{bmatrix} \Delta P_k \\ \Delta Q_k \end{bmatrix}^{(r)} = \begin{bmatrix} 0 & 0 \\ 0 & \frac{2V_k^2}{\pi X_L} \{\cos{(2\alpha_{svc})} - 1\} \end{bmatrix}^{(r)} \begin{bmatrix} \Delta \delta_k \\ \Delta \alpha_{svc} \end{bmatrix}^{(r)}$$
(58)
$$\alpha_{svc}^{(r)} = \alpha_{svc}^{(r-1)} + \alpha_{svc}^{(r)}$$
(59)

Where:

 X_L is the inductive reactance;

 X_C is the capacitive reactance;

 \propto_{svc} is the firing angle of the SVC

 $\Delta \propto_{svc}$ is the firing angle mismatch of the SVC

Modeling and Formulation of Power Flow of Thyristor Controlled Series Compensation (TCSC

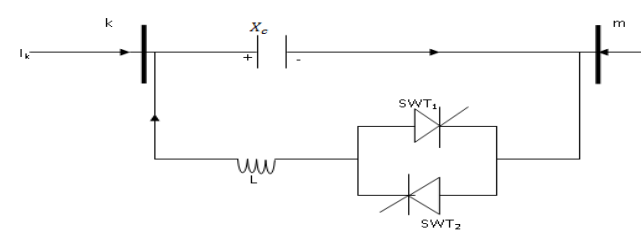


Figure 3: TCSC configuration

Figure 3 shows the TCSC integrated between bus k and bus m. The transfer admittance matrix of the variable series compensator and the active and reactive power equations at bus k and m are given by

$$\begin{bmatrix} I_k \\ I_m \end{bmatrix} = \begin{bmatrix} jB_{KK} & jB_{km} \\ jB_{mk} & jB_{mm} \end{bmatrix} \begin{bmatrix} V_k \\ V_m \end{bmatrix}$$

(60)

At bus k,

$$P_k = V_k V_m B_{km} \sin (\theta_K - \theta_M)$$
(61)
$$Q_K = -V_k^2 B_{kk} - V_k V_m B_{km} \cos (\theta_k - \theta_m)$$
(62)

At bus m,

$$P_m = V_m V_k B_{mk} \sin \left(\theta_m - \theta_k\right)$$
 (63)

$$Q_m = -V_m^2 B_{mm} - V_m V_k B_{mk} \cos \left(\theta_m - \theta_k\right)$$
 (64)

Where;

 I_k is the current at bus k; I_m is the current at bus m;

$$V_k$$
 is the voltage at bus k; V_m is the voltage at bus m;
$$B_{kk} = B_{mm} = -\frac{1}{X_{TCSC}}$$

$$(65)$$

$$B_{km} = B_{mk} = \frac{1}{X_{TCSC}}$$

$$(66)$$

$$X_{TCSC} = -X_C + C_1 \{ 2(\pi - \alpha) + \sin[2(\pi - \alpha)] \} - C_2 \cos^2(\pi - \alpha) \{ \omega \tan[\omega(\pi - \alpha)] - \tan(\pi - \alpha) \}$$

$$(67)$$

For the case when the TCSC controls active power flowing from bus k to bus m at a specified value, the set of linearized power flow equation is

$$\begin{bmatrix} \Delta P_{k} \\ \Delta P_{m} \\ \Delta Q_{k} \\ \Delta Q_{m} \\ \Delta P_{km}^{aTCSC} \end{bmatrix} = \begin{bmatrix} \frac{\partial P_{k}}{\partial \theta_{k}} & \frac{\partial P_{k}}{\partial \theta_{m}} & \frac{\partial P_{k}}{\partial V_{k}} V_{k} & \frac{\partial P_{k}}{\partial V_{m}} V_{m} & \frac{\partial P_{k}}{\partial \alpha} \\ \frac{\partial P_{m}}{\partial \theta_{k}} & \frac{\partial P_{m}}{\partial \theta_{m}} & \frac{\partial P_{m}}{\partial V_{k}} V_{k} & \frac{\partial P_{m}}{\partial V_{m}} V_{m} & \frac{\partial P_{m}}{\partial \alpha} \\ \frac{\partial Q_{k}}{\partial \theta_{k}} & \frac{\partial Q_{k}}{\partial \theta_{m}} & \frac{\partial Q_{k}}{\partial V_{k}} V_{k} & \frac{\partial Q_{m}}{\partial V_{m}} V_{m} & \frac{\partial Q_{k}}{\partial \alpha} \\ \frac{\partial Q_{m}}{\partial \theta_{k}} & \frac{\partial Q_{m}}{\partial \theta_{m}} & \frac{\partial Q_{m}}{\partial V_{k}} V_{k} & \frac{\partial Q_{m}}{\partial V_{m}} V_{m} & \frac{\partial Q_{m}}{\partial \alpha} \\ \frac{\partial Q_{m}}{\partial \theta_{k}} & \frac{\partial Q_{m}}{\partial \theta_{m}} & \frac{\partial Q_{m}}{\partial V_{k}} V_{k} & \frac{\partial Q_{m}}{\partial V_{m}} V_{m} & \frac{\partial Q_{m}}{\partial \alpha} \\ \frac{\partial Q_{m}}{\partial \theta_{k}} & \frac{\partial Q_{m}}{\partial \theta_{m}} & \frac{\partial Q_{m}}{\partial V_{k}} V_{k} & \frac{\partial Q_{m}}{\partial V_{m}} V_{m} & \frac{\partial Q_{m}}{\partial \alpha} \\ \frac{\partial Q_{m}}{\partial \theta_{k}} & \frac{\partial Q_{m}}{\partial \theta_{m}} & \frac{\partial Q_{m}}{\partial V_{k}} V_{k} & \frac{\partial Q_{m}}{\partial V_{m}} V_{m} & \frac{\partial Q_{m}}{\partial \alpha} \\ \frac{\partial Q_{m}}{\partial \alpha} & \frac{\partial Q_{m}}{\partial \theta_{m}} & \frac{\partial Q_{m}}{\partial V_{k}} V_{k} & \frac{\partial Q_{m}}{\partial V_{m}} V_{m} & \frac{\partial Q_{m}}{\partial \alpha} \\ \frac{\partial Q_{m}}{\partial \alpha} & \frac{\partial Q_{m}}{\partial \theta_{m}} & \frac{\partial Q_{m}}{\partial V_{k}} V_{k} & \frac{\partial Q_{m}}{\partial V_{m}} V_{m} & \frac{\partial Q_{m}}{\partial \alpha} \\ \frac{\partial Q_{m}}{\partial \alpha} & \frac{\partial Q_{m}}{\partial \alpha} & \frac{\partial Q_{m}}{\partial \gamma_{k}} V_{k} & \frac{\partial Q_{m}}{\partial \gamma_{m}} V_{m} & \frac{\partial Q_{m}}{\partial \alpha} \\ \frac{\partial Q_{m}}{\partial \gamma_{m}} & \frac{\partial Q_{m}}{\partial \gamma_{m}} V_{m} & \frac{\partial Q_{m}}{\partial \alpha} \\ \frac{\partial Q_{m}}{\partial \gamma_{m}} & \frac{\partial Q_{m}}{\partial \gamma_{m}} V_{m} & \frac{\partial Q_{m}}{\partial \alpha} \\ \frac{\partial Q_{m}}{\partial \gamma_{m}} & \frac{\partial Q_{m}}{\partial \gamma_{m}} & \frac{\partial Q_{m}}{\partial \gamma_{m}} V_{m} & \frac{\partial Q_{m}}{\partial \gamma_{m}} V_{m} \\ \frac{\partial Q_{m}}{\partial \gamma_{m}} & \frac{\partial Q_{m}}{\partial \gamma_{m}} & \frac{\partial Q_{m}}{\partial \gamma_{m}} V_{m} & \frac{\partial Q_{m}}{\partial \gamma_{m}} V_{m} \\ \frac{\partial Q_{m}}{\partial \gamma_{m}} & \frac{\partial Q_{m}}{\partial \gamma_{m}} & \frac{\partial Q_{m}}{\partial \gamma_{m}} V_{m} & \frac{\partial Q_{m}}{\partial \gamma_{m}} V_{m} \\ \frac{\partial Q_{m}}{\partial \gamma_{m}} & \frac{\partial Q_{m}}{\partial \gamma_{m}} & \frac{\partial Q_{m}}{\partial \gamma_{m}} V_{m} & \frac{\partial Q_{m}}{\partial \gamma_{m}} V_{m} \\ \frac{\partial Q_{m}}{\partial \gamma_{m}} & \frac{\partial Q_{m}}{\partial \gamma_{m}} & \frac{\partial Q_{m}}{\partial \gamma_{m}} V_{m} & \frac{\partial Q_{m}}{\partial \gamma_{m}} V_{m} \\ \frac{\partial Q_{m}}{\partial \gamma_{m}} & \frac{\partial$$

Where ΔP , ΔQ , $\Delta P_{km}^{\alpha TCSC}$ constitute the power mismatch equation and these are expressed as:

$$\begin{array}{l} \Delta P_{k} = P_{gk} - P_{lk} - P_{k}^{cal} = P_{k}^{sch} - P_{k}^{cal} = 0 \\ (69) \\ \Delta Q_{k} = Q_{gk} - Q_{lk} - Q_{k}^{cal} = Q_{k}^{sch} - Q_{k}^{cal} = 0 \\ (70) \\ \Delta P_{km}^{\sim TCSC} = P_{km}^{reg} - P_{km}^{\sim TCSC,cal} \\ \end{array}$$

Where

 P_{km}^{reg} is the active power to be controlled from bus k to bus m:

 $P_{km}^{\propto TCSC,cal}$ is the calculated active power of the TCSC at bus k.

Similarly, $\Delta\theta$, ΔV , $\Delta\alpha^{TCSC}$ are the state variable and expressed as:

$$\Delta\theta = \theta^{i+1} - \theta^{i}$$
(72)
$$\Delta V = V^{i+1} - V^{i}$$
(73)
$$\Delta \propto^{TCSC} = \propto^{TCSC} (i+1) - \propto^{TCSC} (i)$$
(74)

 $\Delta \propto^{TCSC}$ is the incremental change in the TCSC firing angle at the i^{th} iteration.

The Jacobian elements for the series resistance as a function of the firing angle \propto_{TCSC} are expressed as a partial derivative of the variable series impedance model and partial derivative of the firing angle model below:

Partial derivative of the variable series impedance model:

$$\frac{\partial P_k}{\partial X}X = -V_k V_m B_{km} \sin (\theta_k - \theta_m) \quad (75)$$

$$\frac{\partial Q_k}{\partial X}X = -V_K^2 B_{KK} - V_K V_M B_{KM} \cos (\theta_K - \theta_M)$$

$$(76)$$

$$\frac{\partial P_{km}}{\partial X}X = \frac{\partial P_k}{\partial X}X \quad (77)$$
Partial derivative of the firing angle model:

Tartial derivative of the filling angle mode
$$\frac{\partial P_k}{\partial \alpha} = P_k B_{TCSC} \frac{\partial X_{TCSC}}{\partial \alpha}$$

$$(78)$$

$$\frac{\partial Q_k}{\partial \alpha} = Q_k B_{TCSC} \frac{\partial X_{TCSC}}{\partial \alpha}$$

$$(79)$$

$$\frac{\partial B_{TCSC}}{\partial \alpha} = B_{TCSC}^2 \frac{\partial X_{TCSC}}{\partial \alpha}$$

$$(80)$$

$$\frac{\partial X_{TCSC}}{\partial \alpha} = -2C_1 [1 + \cos(2 \propto)] + C_2 \sin(2 \propto) \{\omega \tan[\omega(\pi - \infty)] - \tan \infty\} + C_2 \left\{\omega^2 \frac{\cos^2(\pi - \infty)}{\cos^2[\omega(\pi - \infty)} - 1\right\}$$

Modeling and Formulation of Power Flow of Static Synchronous Compensator (STATCOM)

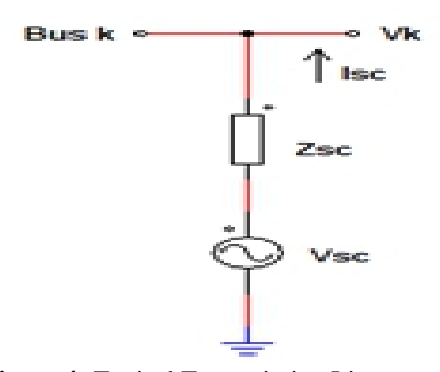


Figure 4: Typical Transmission Line

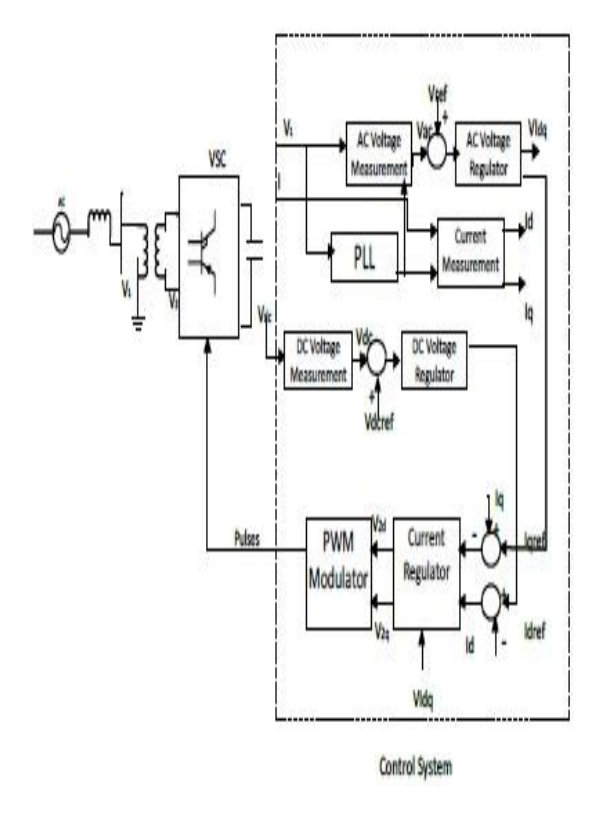


Figure 5: An equivalent circuit of a voltage source converter.

The STATCOM model equations are written as follows:

$$P_{sc} = V_{sc}I_{sc}$$
(66)
$$P_k = V_kI_{sc}$$
(67)

Subject to constrain,

$$V_{sc(min)} \le V_{sc} \le V_{sc(max)}$$
(68)

The switch mode voltage converter and its transformer are given by

$$V_{sc} = V_k + Z_{sc}I_{sc}$$
(69)

$$Z_{sc} = (R_{sc} + X_{sc})^{1/2}$$
(70)
$$Y_{sc} = \frac{1}{Z_{sc}} \qquad (71)$$

$$V_{k(Equivalent)} = \sum_{k=1}^{n} V_{k}$$
(72)
$$V_{k} = e_{k} + jf_{k} \qquad (73)$$

$$V_{sc} = e_{sc} + jf_{k} \qquad (74)$$

$$|V_{sc}| = (e_{sc}^{2} + f_{sc}^{2})^{1/2} \qquad (75)$$

$$\delta_{k} = \tan^{-1} \left(\frac{f_{sc}}{e_{sc}}\right) \qquad (76)$$

Where;

 P_{sc} and P_k are the active power injected into bus K by VSC; $|V_{sc}|$

 $V_{sc(min)}$ and $V_{sc(max)}$ are STATCOM minimum and maximum AC voltage;

 Z_{sc} and Y_{sc} are the coupling transformer impedance and short circuit admittance respectively;

 V_k is the voltage at bus K;

 V_{sc} is the voltage source converter voltage;

 $|V_{sc}|$ and δ_k are the STATCOM voltage magnitude and angle respectively;

 e_k and f_k are the real and imaginary part of bus voltage; e_{sc} and f_{sc} are the real and imaginary part of the STATCOM voltage.

Assuming that the STATCOM is operating in voltage control mode, it absorbs proper amount of reactive power from the power system to keep $|V_{sc}|$ constant for all power system loading within reasonable range. The ohmic loss of the STATCOM is accounted by considering the real part of Y_{start} in power flow calculations. The power flow equation of the net active and reactive power injection at bus K can be written as follows:

$$P_{k} = P_{stat} + \sum_{j=1}^{n} |V_{k}| |V_{j}| |Y_{kj}| \cos(\delta_{k} - \delta_{j} - \theta_{kj})$$
(77)
$$Q_{k} = Q_{stat} + \sum_{j=1}^{n} |V_{k}| |V_{j}| |Y_{kj}| \sin(\delta_{k} - \delta_{j} - \theta_{kj})$$
(78)
$$P_{stat} = G_{stat} + \sum_{j=1}^{n} |V_{k}|^{2} - |V_{k}| |E_{stat}| |Y_{stat}| \cos(\delta_{k} - \delta_{stat} - \theta_{stat})$$
(79)
$$Q_{stat} = B_{stat} + \sum_{j=1}^{n} |V_{k}|^{2} - |V_{k}| |E_{stat}| |Y_{stat}| \sin(\delta_{k} - \delta_{stat} - \theta_{stat})$$
(80)
$$PE_{stat} = Real[E_{stat}I_{stat}] = -G_{stat}|E_{stat}|^{2} + |V_{k}||E_{stat}| |Y_{stat}| \cos(\delta_{k} - \delta_{j} - \theta_{stat}) = 0$$
(81)

Using the power equations along with the linearized Newton Raphson power flow equation for this model we have;

$$\begin{bmatrix} \Delta P_{k} \\ \Delta Q_{k} \\ \Delta P_{stat} \\ \Delta Q_{stat} \end{bmatrix} = \begin{bmatrix} \frac{\partial P_{k}}{\partial \theta_{k}} & \frac{\partial P_{k}}{\partial V_{k}} V_{k} & \frac{\partial P_{k}}{\partial \theta_{stat}} \frac{\partial P_{k}}{\partial V_{stat}} V_{stat} \\ \frac{\partial Q_{k}}{\partial \theta_{k}} & \frac{\partial Q_{k}}{\partial V_{k}} V_{k} & \frac{\partial Q_{k}}{\partial \theta_{stat}} \frac{\partial Q_{k}}{\partial V_{stat}} V_{stat} \\ \frac{\partial P_{stat}}{\partial \theta_{k}} & \frac{\partial P_{stat}}{\partial V_{k}} V_{k} & \frac{\partial P_{stat}}{\partial \theta_{stat}} \frac{\partial P_{stat}}{\partial V_{stat}} V_{stat} \\ \frac{\partial Q_{stat}}{\partial \theta_{k}} & \frac{\partial Q_{stat}}{\partial V_{k}} V_{k} & \frac{\partial Q_{stat}}{\partial \theta_{stat}} \frac{\partial P_{stat}}{\partial V_{stat}} V_{stat} \\ \frac{\partial Q_{stat}}{\partial \theta_{k}} & \frac{\partial Q_{stat}}{\partial V_{k}} V_{k} & \frac{\partial Q_{stat}}{\partial \theta_{stat}} & \frac{\partial Q_{stat}}{\partial V_{stat}} V_{stat} \end{bmatrix} \begin{bmatrix} \Delta \theta_{k} \\ \frac{\Delta V_{k}}{V_{k}} \\ \frac{\Delta V_{k}}{V_{k}} \\ \frac{\Delta V_{k}}{\partial \theta_{stat}} & \frac{\partial V_{k}}{\partial V_{stat}} V_{stat} \\ \frac{\partial V_{k}}{\partial V_{stat}} & \frac{\partial V_{k}}{\partial V_{stat}} & \frac{\partial V_{k}}{\partial V_{stat}} & \frac{\partial V_{k}}{\partial V_{stat}} & \frac{\partial V_{k}}{\partial V_{stat}} \\ \frac{\partial V_{k}}{\partial V_{k}} & \frac{\partial V_{k}}{\partial V_{k$$

III. RESULT AND DISCUSSION

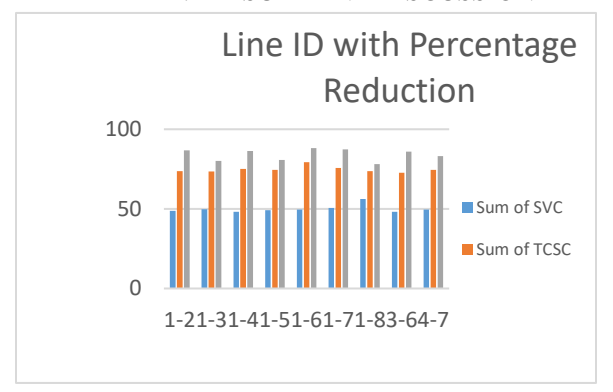


Figure 6: Graphical representation of Power loss reduction without and with SVC, TCSC, STATCOM

With placement of SVC, TCSC and STATCOM one after the other on the weakest bus, slight increase of percentage voltage on the buses were noticed with SVC and TCSC while with STATCOM, higher percentage increase was recorded where BUS-3 (AFAM) and BUS-30 (JALINGO) has the highest increase of 98.34% and 98.13% respectively as shown in Figure 6.

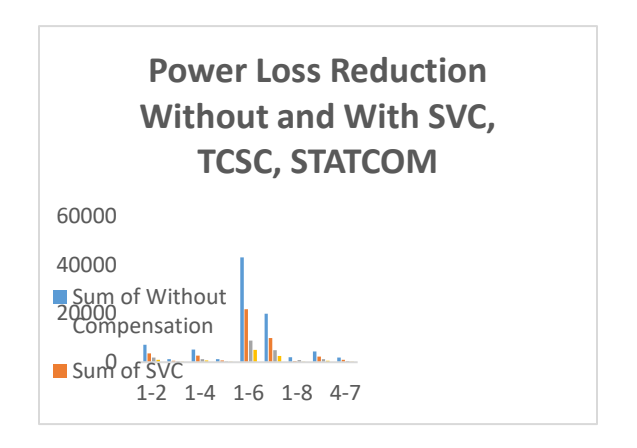


Figure 7: Graphical representation of percentage loss reduction with SVC, TCSC, STATCOM

In power lose reduction with compensation; TCSC and STATCOM recorded higher percentage reduction of power compared to SVC with 79.4% and

88.2% at line 1-6 as shown in Figure 7. Power lose reduction. This implies that STATCOM gives better voltage stability enhancement and power lose reduction

IV. CONCLUSION

Today, voltage instability and power loose reduction have become two important factors that are affecting the performance of power transmission systems. In this regard, FACTS devices have shown better ways for maintaining and improving voltage stability during load variation.

This paper had discussed the features; application and comparison of SVC, TCSC and STATCOM as compensating devices in enhancing voltage stability and power lose reduction of 52 bus transmission system, where each of the devices was attached to the weakest bus and simulation carried out on application of Newton Raphson load flow method. The obtained result from the test system without and with the proposed FACTS devices using MATLAB/ETAP software revealed that STATCOM had the highest increase of the percentage bus voltage while TCSC and STATCOM have highest power

References

- [1] A. B. Abdullah, M. Mehdi, and B. K. Azhar, "Comprehensive Comparison of FACTS Devices for Enhancing Static Voltage Stability," *ARPN Journal of Engineering and Applied Science*, vol. 11, no. 2, pp. 12602–12606, 2016.
- [2] G. Abhishek and S. Balwinder, "Impact of FACTS Technology: A State of Art Review," *International Journal of Innovative Technology and Exploring Engineering*, vol. 1, no. 4, pp. 114–120, 2012.
- [3] I. G. Adebayo, I. A. Adejumobi, and O. S. Olajire, "Power Flow Analysis and Voltage Stability Enhancement Using Thyristor Controlled Series Capacitor (TCSC) FACTS Controller," *International Journal of Engineering and Advanced Technology*, vol. 2, no. 3, pp. 100–105, 2013.
- [4] O. I. Adebisi, I. A. Adejumobi, and P. E. Ogunbowale, "Application of Static Var Compensator for Voltage Stability Enhancement and Power Loss Reduction in Power System," *LAUTECH Journal of Engineering and Technology*, vol. 11, no. 2, pp. 46–58, 2017.
- [5] I. A. Adejumobi and P. E. Ogunbowale, "Comparative Analysis of FACTS Devices for Voltage Stability Enhancement and Power Loss Reduction in

- Power System Network," *LAUTECH Journal of Engineering and Technology*, vol. 14, no. 2, pp. 167–179, 2020.
- [6] O. A. Adeniji and P. O. Mbamaluikem, "Voltage Stability Enhancement and Efficiency Improvement of Nigeria Transmission System Using Unified Power Flow Controller (UPFC)," *American Journal of Engineering Research*, vol. 6, no. 1, pp. 37–43, 2017.
- [7] G. A. Adepoju and O. A. Komolafe, "Power Injection Model and High Voltage DC-Voltage Source Converter for Power Analysis," in *Proc. Int. Conf. Power System Analysis, Control and Optimization*, vol. 8, no. 2, pp. 67–72, 2011.
- [8] M. Alinezhad and H. Lesani, "Comparison of SVC, TCSC and UPEC Controllers for Static Voltage Stability Evaluation by Continuation Power Flow Method," *International Journal of Engineering Research and Technology*, vol. 4, no. 4, pp. 339–344, 2015.
- [9] K. Alock and D. Sury, "Enhancement of Transient Stability in Transmission Line Using SVC-FACTS Controller," *International Journal of Recent Technology and Engineering*, vol. 2, no. 2, pp. 111–118, 2013.
- [10] K. M. Alok and B. K. Amar, "Power System Stability Improvement Using the FACTS Devices," *International Journal of Modern Engineering Research*, vol. 1, no. 2, pp. 666–672, 2012.
- [11] G. Amit and K. A. Sanjai, "Modeling and Simulation of SVC for Improvement of Voltage Stability in Power System," *International Journal of Electronics, Communication and Computer Engineering*, vol. 2, no. 2, pp. 202–204, 2011.
- [12] A. Anbarasan and M. Sanavullah, "Voltage Stability Improvement in Power System Using STATCOM," *International Journal of Engineering Science and Technology*, vol. 4, no. 11, pp. 4585–4591, 2012.
- [13] C. H. Apribowo, O. Listiyanto, and M. H. Ibrahim, "Placement of Static Var Compensator (SVC) for

- Improving Voltage Stability Based on Sensitivity Analysis: A Case Study of 500KV Java-Bali Electrical Power System," in 6th Int. Conf. Electric Vehicular Technology, pp. 276–280, 2019.
- [14] A. E. Apriyato, A. R. Virgiawan, and H. Pariaman, "Determination of Var Compensator Placement for System Stability Improvement on Java Bali Network," *IOP Conf. Ser. Mater. Sci. Eng.*, vol. 1096, no. 1, pp. 121–133, 2021.
- [15] S. Arthit and M. Hadarajah, "Static Voltage Stability Margin Enhancement Using STATCOM, TCSC and SSSC," in *IEEE/PES Transm. and Distrib. Conf. and Exhibition*, pp. 1–6, 2005.
- [16] V. Asha and S. Padma, "Maintaining Voltage Stability in Power System Using FACTS Devices," *International Journal of Engineering, Science and Invention (IJEST)*, vol. 2, no. 2, pp. 20–25, 2013.
- [17] M. Asma and C. Souad, "Heuristic-Based Approach for Voltage Stability Improvement Using FACTS Devices," *Advances in Science, Technology and Engineering System Journal*, vol. 2, no. 6, pp. 252–260, 2017.
- [18] A. J. Atuchukwu, I. I. Okonkwo, and E. O. Okoye, "Voltage Stability Enhancement Using Static Var Compensator (SVC)," *International Research Journal of Modernization in Engineering Technology and Science*, vol. 4, no. 4, pp. 2582–5208, 2022.
- [19] V. A. Avneesh and S. Dhaneshwari, "Efficient Voltage Regulation in Three Phase AC Transmission Line Using Static Var Compensator (SVC)," *International Journal of Advanced Research in Electrical, Electronic and Instrumentation Engineering*, vol. 10, no. 3, pp. 60–66, 2013.
- [20] P. Bahadur and B. Sumam, "Power Flow Model of SVC and STATCOM," *International Journal Advanced Engineering and Technology*, vol. 9, no. 3, pp. 120–130, 2017.